

E19-2014-48

M. Batmunkh<sup>1,2</sup>, O. Belov<sup>1</sup>, O. Lhagva<sup>2</sup>,  
L. Bayarchimeg<sup>1</sup>, P. Battogtokh<sup>2</sup>

SIMULATION OF ENERGY DEPOSITION FROM  $^{125}\text{I}$  AND  
 $^{213}\text{Bi}$  DECAYS IN THE CELL NUCLEUS

---

<sup>1</sup> Joint Institute for Nuclear Research, Dubna

<sup>2</sup> Department of Theoretical Physics, National University of Mongolia,  
Ulaanbaatar

Батмунх М. и др.

E19-2014-48

Моделирование энерговыделения в распадах  $^{125}\text{I}$  и  $^{213}\text{Bi}$ ,  
происходящих в ядре клетки

Выполнено моделирование распадов радионуклидов  $^{125}\text{I}$  и  $^{213}\text{Bi}$ , происходящих в сферическом объеме, соответствующем размеру ядра клетки. С использованием подхода, основанного на расчете структуры трека испускаемых частиц методом Монте-Карло, оценены радиальное распределение переданной энергии и спектры кинетической энергии электронов, возникающих в распадах. Учет возможности повреждения ДНК клеток выполнен путем кластерного анализа структуры треков испускаемых частиц в объемах, соответствующих диаметру нативной двунитевой ДНК. Для этой цели использован модельный подход, основанный на совместном применении программных пакетов *G4-RadioactiveDecay* и *G4-DNA* системы моделирования Geant4.

Работа выполнена в Лаборатории радиационной биологии ОИЯИ.

Сообщение Объединенного института ядерных исследований. Дубна, 2014

Batmunkh M. et al.

E19-2014-48

Simulation of Energy Deposition from  $^{125}\text{I}$  and  $^{213}\text{Bi}$  Decays  
in the Cell Nucleus

We modeled the radioactive decays of  $^{125}\text{I}$  and  $^{213}\text{Bi}$  radionuclides inside the spherical volume simulating a cell nucleus. Using the Monte-Carlo-based track structure simulation technique, we estimated the radial distribution of deposited energy and the kinetic energy spectra of electrons produced by primary particles resulting from decay. To address the possibility of DNA damage, we performed the cluster analysis of track structures of emitted particles inside the volumes corresponding to the diameter of the native double-stranded DNA. For this purpose, *G4-RadioactiveDecay* and *G4-DNA* program packages from the Geant4 Monte Carlo toolkit were combined together.

The investigation has been performed at the Laboratory of Radiation Biology, JINR.

Communication of the Joint Institute for Nuclear Research. Dubna, 2014

## INTRODUCTION

Precise estimation of energy deposition in malignant cells plays a crucial role in nuclide diagnostics and therapy. Nowadays Monte Carlo technique has turned out to be a useful and common applicable method for simulation of radiation transport in relatively small volumes corresponding to the size of the cell nucleus [1–3]. In particular, these estimations can be important in two-step targeting, which becomes a promising approach in cancer treatment enabling to deliver the toxic substance to the nucleus of the cell [4]. In this regard, simulation of the energy deposition from radionuclides transmitted inside the cell nucleus is required for the correct estimation of DNA damage resulting from nuclide decay.

In this work, we simulated the decays of Iodine ( $^{125}\text{I}$ ) and Bismuth ( $^{213}\text{Bi}$ ) radionuclides inside the spherical model of the cell nucleus. For this purpose, we integrated *G4-DNA* low-energy electromagnetic package with the *G4-RadioactiveDecay* model at nuclear level, which are both fully included in Geant4 toolkit [5, 6]. The radionuclide  $^{125}\text{I}$  is mainly used for treating thyroid cancer and imaging the thyroid at higher abundance [7–10].  $^{125}\text{I}$  with the half-life of 59.4 d emits electrons and photons producing the daughter  $^{125}\text{Te}$  (Tellurium) nuclide with the energy of 35.4 keV. Since  $^{125}\text{Te}$  is an excited state possessing the half-life of  $1.6 \cdot 10^{-9}$  s, it undergoes further decay proceeding to the stable state of nonradioactive  $^{125}\text{Te}$  nuclide with zero energy. This transition is characterized by 7% of gamma emission and 93% of internal conversion. An example of  $^{125}\text{I}$  radioactive decay is shown in Fig. 1, *a*. The second radionuclide  $^{213}\text{Bi}$  is a radioisotope also commonly used for nuclear medicine. In fact, it is used in radioimmunology to treat patients with leukemia, lymphomas, as well as for micrometastatic carcinomas [11]. It has unique nuclear properties such as a short 45-minutes half-life and high-energy (around 8.4 MeV) alpha-particle emission with a high linear energy transfer. A scheme of the  $^{213}\text{Bi}$  radionuclide decay is shown in Fig. 1, *b*. In this decay chain,  $^{213}\text{Bi}$  (83 protons, 130 neutrons) disintegrates about 98% by 444 keV electron (beta-minus) emission resulting in  $^{213}\text{Po}$  (84 protons, 129 neutrons) and about 2% through the alpha decay with energy of 5.9 MeV resulting in  $^{209}\text{Tl}$  (81 protons, 128 neutrons). The daughter  $^{213}\text{Po}$  and  $^{209}\text{Tl}$  nuclides are the excited states with the half-life of 4.2  $\mu\text{s}$  and 2.2 min. At the next step, these nuclides transform to the unstable  $^{209}\text{Pb}$  (82 pro-

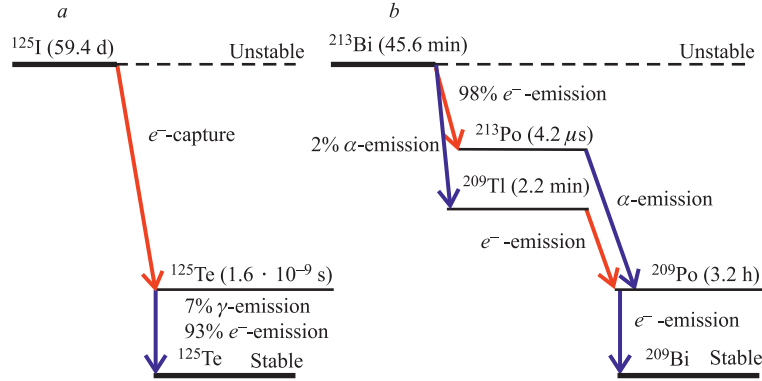


Fig. 1. Decay schemes of  $^{125}\text{I}$  (a) and  $^{213}\text{Bi}$  (b) radionuclides

tons, 127 neutrons) by alpha and beta emission with energies of 8.4 MeV and 659 keV, respectively. Finally,  $^{209}\text{Pb}$  decays to the nonradioactive stable  $^{209}\text{Bi}$  (83 protons, 126 neutrons) by emission of 198 keV beta particles.

## 1. METHODS

**1.1. Simulation of the Radioactive Decays.** Radioactive decay is a stochastic physics process where an atom with unstable nuclei transmutes into daughter nuclides losing or gaining a neutron or a proton. This physics process does not require external interactions for decays schemes mentioned in Fig. 1.

Monte-Carlo-based technique for simulation of radioactive decay is available in the extended example named ‘*rdecay01*’ of Geant4 toolkit. It is based on data taken from Evaluated Nuclear Structure Data File (ENSDF) [12]. This example demonstrates the use of some basic features of *G4-RadioactiveDecay* hadronic package, which allows displaying counts of created particles, their kinetic energies, time of life, and activity of individual decays [13]. In the present study, we have integrated a simple spherical model of the tumor cell nucleus with the radius of  $1\ \mu\text{m}$  to this Geant4 code. The radionuclide was placed in the center of cell nucleus.

**1.2. Track Structure Calculations and Cluster Analysis.** The track structures of particles emitted in  $^{125}\text{I}$  and  $^{213}\text{Bi}$  radioactive decays are calculated by the *G4-DNA* low-energy electromagnetic package assuming the random distribution of the particles inside the cell nucleus. The *G4-DNA* package is an extension of standard Geant4 toolkit for simulating the physical and radiobiological processes at cellular and nanometric levels [5, 6]. The physics of atomic interaction is characterized by the processes of ionization, excitation (electronic and vibrational), molecular attachment, and elastic scattering for emitted electrons, and by photoelectric effect, Compton and Rayleigh scattering, and gamma conversion — for

photons. Ionization, excitation, and charge transfer are taken into account for emitted protons and alpha particles. Decays of both radionuclides are simulated with lower cutoff energies of 4 eV for electrons.

In our simulation, spatial energy depositions from the stochastic traveling emitted particles are defined in the points with coordinates corresponding to each particle interaction in the cell nucleus. This allows estimating the distribution of energy depositions along the radius of nucleus, as well as the energy spectrum of emitted particles and distribution of the specific energy. The specific energy  $z$ , which is also sometimes called deposited dose in cell nucleus, can be calculated by  $z = \varepsilon_i / \rho V$ , where  $\varepsilon_i$  is the energy imparted by the  $i$ th emitted particle ( $\varepsilon_i > 0$ ) to matter of the density  $\rho$  in the volume  $V$  [14]. In our calculations,  $\rho$  is the density of liquid water equaling to  $1 \text{ g} \cdot \text{cm}^{-3}$  and  $V$  is the volume of spherical phantom representing the cell nucleus ( $V = 4.18 \mu\text{m}^3$ ).

To address the possibility of DNA damage, we also performed the cluster analysis of track structures of emitted particles at nanometer scale. For this purpose, we used the cluster analyzing algorithm developed earlier [15]. The diameter of all produced clusters was set to be 2 nm that corresponds to the diameter of the native double-stranded DNA. This enables estimating the frequency distribution of particles affecting DNA and calculating the number of DNA segments hit by particles.

## 2. RESULTS AND DISCUSSION

**2.1. Track Structures of  $^{125}\text{I}$  and  $^{213}\text{Bi}$ .** For estimation of quantities referred to energy deposition, we simulated track structures of 1000 decays from each of two radionuclides. An example of these simulations for the lesser number of

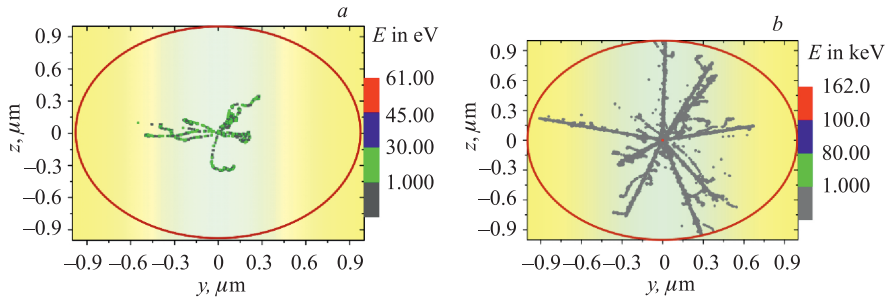


Fig. 2. The  $yz$  projections of track structures of 10  $^{125}\text{I}$  (a) and 10  $^{213}\text{Bi}$  (b) decays as calculated with the *G4-DNA* package. Circles represent the cell nucleus of  $2 \mu\text{m}$  diameter. Dots correspond to events of nonzero energy deposition ( $E_i > 0$ ). The simulation results are represented as the Cartesian coordinates of the produced ionizations. The energy deposited in each event is characterized by the color map and expressed in electron volts (eV) in panel a and in kiloelectron volts (keV) in panel b

events equaling to 10 is shown in Fig. 2. The depicted 10-event track structures are characterized by the numerical results presented in Tables 1–3. The parameters which were scored include the total  $E$  and mean  $\bar{E}$  energies of emitted particles, the numbers  $N_I$  and  $N_{Bi}$  of physical processes generated during calculations

**Table 1. The number of emitted particles generated during calculations and their mean energy**

Type of the particle	$^{125}\text{I}$		$^{213}\text{Bi}$	
	Number of emitted particles	Mean energy of emitted particles, keV	Number of emitted particles	Mean energy of emitted particles, keV
$e^-$	1694	0.056	28658	0.24
$\gamma$	1	35.49	3	440.5
$\nu_{e^-}$	10	150.3	–	–
$\bar{\nu}_{e^-}$	–	–	20	656.6
$\alpha$	–	–	12	8368
$\alpha^+$	–	–	2	8325
He	–	–	1	8365

**Table 2. The number of physical processes generated by Geant4 for the emitted particles**

Process name	Number of processes	
	$^{125}\text{I}$	$^{213}\text{Bi}$
<i>RadioactiveDecay</i>	24	39
<i>Transportation</i>	12	77
<i><math>e^-</math>_GADN AIonisation</i>	1685	19035
<i><math>e^-</math>_GADN AElastic</i>	86245	1245054
<i><math>e^-</math>_GADN AExcitation</i>	225	3169
<i><math>e^-</math>_GADN AVibExcitation</i>	9721	140212
<i><math>e^-</math>_GADN AAttachment</i>	31	437
<i><math>\alpha</math>_GADN AIonisation</i>	–	9571
<i><math>\alpha</math>_GADN AExcitation</i>	–	802
<i><math>\alpha</math>_GADN AChargeDecrease</i>	–	2
<i><math>\alpha^+</math>_GADN AIonisation</i>	–	6
<i><math>\alpha^+</math>_GADN AExcitation</i>	–	4
<i><math>\alpha^+</math>_GADN AChargeIncrease</i>	–	2
<i>He_GADN AIonisation</i>	–	–
<i>He_GADN AChargeIncrease</i>	–	1
<i>He_GADN AExcitation</i>	–	–

**Table 3. Total ( $E$ ) and mean ( $\bar{E}$ ) deposited energy, total ( $z$ ) and mean ( $D$ ) deposited dose, and mean specific activity as estimated in calculations. Specific activity is defined as an activity per unit of mass of the primary radionuclide. Activity of radioactive decay is expressed as the number of atoms that decay per unit of time. The value of radioactive decay is expressed here in Ci (Curie) [ $1 \text{ Ci} = 3.7 \cdot 10^{10} \text{ Bq}$ ]**

Parameter	$^{125}\text{I}$	$^{213}\text{Bi}$
$E$ , keV	29.8	2162.2
$\bar{E}$ , keV	2.98	216.22
$z$ , Gy	1.14	82.71
$D$ , Gy	0.14	8.271
Mean specific activity, Ci/g	$2.23 \cdot 10^4$	$2.65 \cdot 10^7$

of  $^{125}\text{I}$  and  $^{213}\text{Bi}$  decays, respectively, the mean deposited energy expressed in terms of absorbed dose  $D$ , and the total deposited energy represented as the specific energy  $z$ . These estimations are performed using the low-energy electromagnetic packages of *G4-DNA*. The numerical results and plots depicting the track structures were obtained with the ROOT object-oriented data analysis framework [16].

**2.2. Physical Characteristics of  $^{125}\text{I}$  and  $^{213}\text{Bi}$  Decays.** In this subsection, we report the comparison of several physical characteristics of decays of two radionuclides. We calculated the total lifetime of decay chain per event for both radionuclides (Fig. 3) and estimated the kinetic energy spectrum of primary electrons from 1000 decays of each radionuclide (Fig. 4) and the distribution of spatial energy deposition of portion of their electrons emitted only inside the cell nucleus (Fig. 5). In the case of  $^{213}\text{Bi}$ , more electrons of high kinetic and deposited energies are generated, which leads to the shorter lifetime than for  $^{125}\text{I}$ . The results on calculation of the kinetic energy spectrum and the total electron

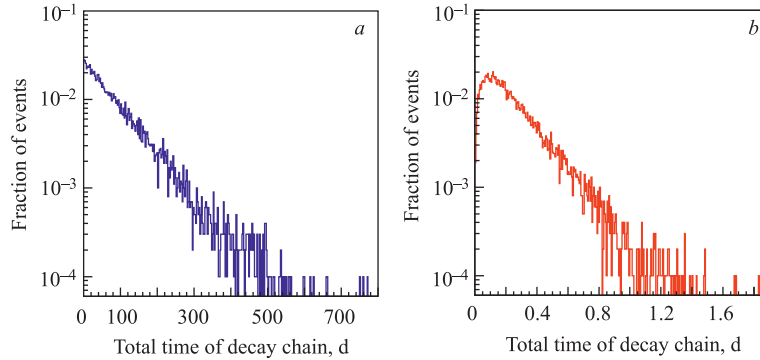


Fig. 3. The total lifetime of decay chain of  $^{125}\text{I}$  (a) and  $^{213}\text{Bi}$  (b) radionuclides

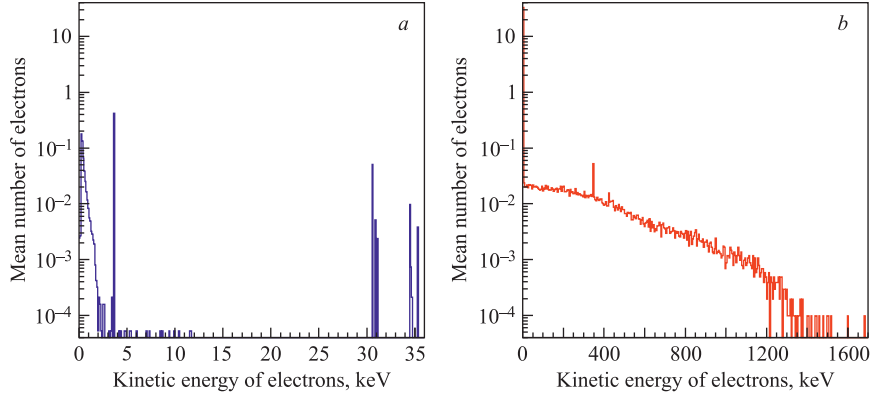


Fig. 4. Kinetic energy spectrum of primary electrons per event of  $^{125}\text{I}$  (a) and  $^{213}\text{Bi}$  (b) decays

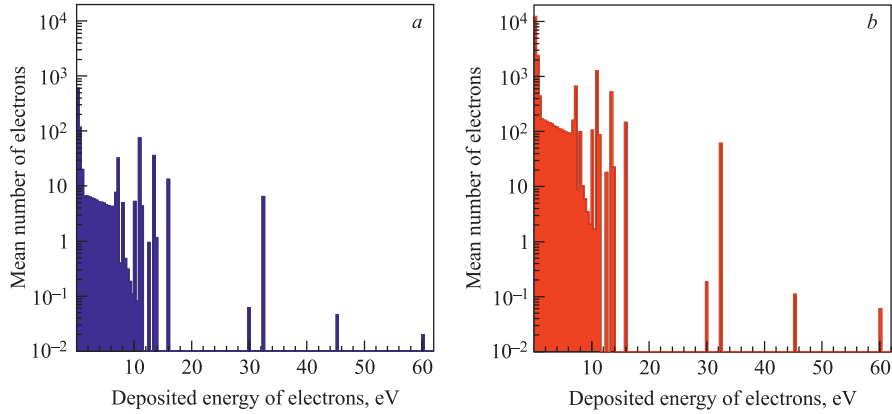


Fig. 5. The spatial distribution of energy deposition per event of emitted electron inside the cell nucleus from  $^{125}\text{I}$  (a) and  $^{213}\text{Bi}$  (b) decays

energy deposition of  $^{125}\text{I}$  decay were compared with the Monte Carlo simulations of other authors [7–9].

Our simulations enabled to obtain the spectrum of specific energy in  $^{125}\text{I}$  and  $^{213}\text{Bi}$  decays inside the cell nucleus (Fig. 6). To estimate the mean specific energy, we applied a Gaussian fit to the computed data. It gave the mean value of  $0.14 \pm 0.02$  Gy for  $^{125}\text{I}$  and  $8.47 \pm 0.03$  Gy for  $^{213}\text{Bi}$  decays. According to definition of the absorbed dose [14], these values can be considered as the dose absorbed inside the cell nucleus. From our estimations it can be also concluded that  $^{125}\text{I}$  may deliver smaller dose with lower probability than  $^{213}\text{Bi}$ .

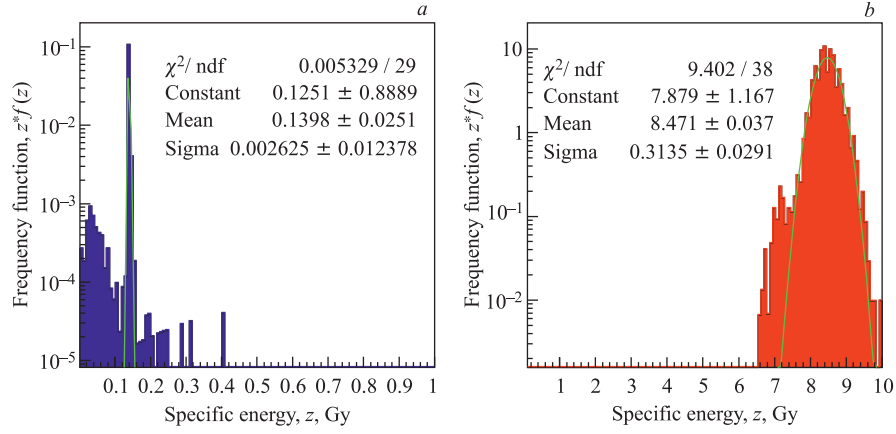


Fig. 6. The spectrum of the specific energy per event in the cell nucleus, adjusted to the Gaussian distribution. Panel *a* shows the distribution for decay of  $^{125}\text{I}$ ; panel *b* represents the distribution for  $^{213}\text{Bi}$  decay

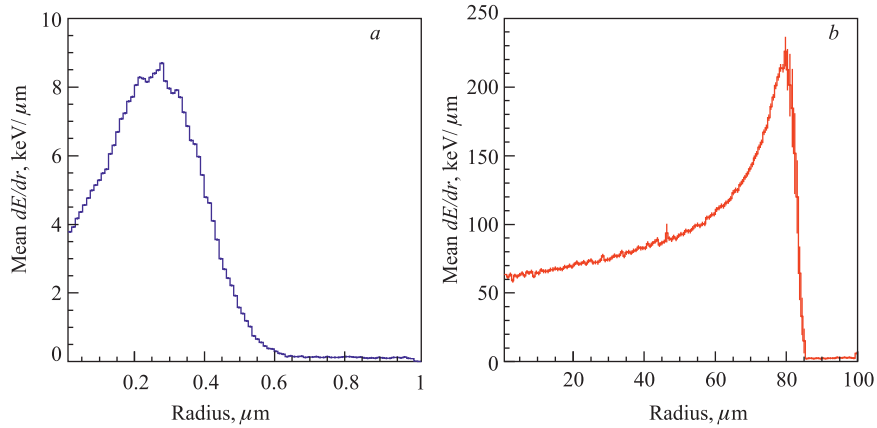


Fig. 7. The radial distribution of energy deposited inside the cell nucleus along trajectories of all emitted particles. The results are represented per event of  $^{125}\text{I}$  (*a*) and  $^{213}\text{Bi}$  (*b*) decays. The radial energy deposition gets more at  $0.3 \mu\text{m}$  in radius for  $^{125}\text{I}$  decays and for  $^{213}\text{Bi}$  decay an increase in ionization density is seen at the end of emitted particles, also known as the Bragg curve, and peak occurs of about  $80 \mu\text{m}$  in radius

In our study, we also computed the radial distribution of energy deposited inside the cell nucleus along all trajectories of incident particles (Fig. 7). Depicted curves characterize the so-called longitudinal energy profile, or depth dose distri-

bution of emitted particles calculated with the *G4-DNA* package. The comparison of the data obtained for two nuclides shows that  $^{125}\text{I}$  delivers the maximal energy at the radius of about  $0.3\ \mu\text{m}$ , while  $^{213}\text{Bi}$  demonstrates a more expanded pattern of energy deposition with the peak within the radius of about  $0.3\ \mu\text{m}$ . Considering the effect from a single nuclide, these facts suggest that  $^{125}\text{I}$  is more convenient to precise killing of individual tumoral cells with minimal damage to neighboring ones, whereas  $^{213}\text{Bi}$  can be effectively used for micrometastases representing larger objects with the radius of up to  $80\ \mu\text{m}$ .

**2.3. Cluster Analysis.** Limiting the space by the size of cell nucleus, we calculated the frequency distribution of cluster sizes from all particles' track structures. Here, the cluster size is considered as the number of ionizations inside the spherical volume equaling to diameter of the native double-stranded DNA. Figure 8, *a* shows the distributions computed for  $^{125}\text{I}$  and  $^{213}\text{Bi}$ . These results show that the most probable cluster size for the concerned nuclides equals to 3 ionizations inside. This is enough to produce more than one complex DNA lesion including double-strand breaks. In this regard, our data are in agreement with the findings reviewed in [17].

Furthermore, the curve obtained for  $^{213}\text{Bi}$  has a pronounced plateau indicating the formation of clusters with the higher number of ionizations equaling to  $\sim 24 - 30$ . In contrast with this,  $^{125}\text{I}$  demonstrates the different pattern of distribution for cluster sizes greater than 20.

Along with the cluster analysis, we estimated the total energy deposited in produced clusters (Fig. 8, *b*). The plot demonstrates that number of created

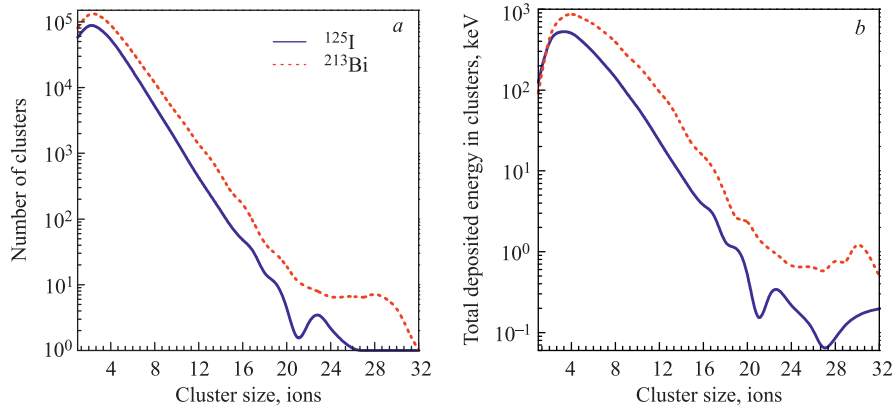


Fig. 8. Cluster size distribution (*a*) and distribution of total energy deposited to each created cluster (*b*) in the case of  $^{125}\text{I}$  and  $^{213}\text{Bi}$ . The cluster diameter is set to be  $2\ \text{nm}$

clusters is directly related to deposited energy in created clusters. Accordingly, decreases energy deposition when increases cluster size, but to compare number of clusters, the broader distributions and highly-localized energy deposition in higher cluster size. In the case of  $^{213}\text{Bi}$ , localized energy deposition is lower on 1–2 ionizations in cluster and also higher-broader distributions appearing in cluster size more than 3 for  $^{125}\text{I}$ .

## CONCLUSIONS

We developed the combined package for simulation of the track structures of particles emitting from radionuclides placed inside a cell nucleus. The simulation code integrates *G4-RadioactiveDecay* and *G4-DNA* subpackages of Geant4 toolkit (version 9.6). Using this approach, we estimated the spatial distribution of energy deposition from decays of  $^{125}\text{I}$  and  $^{213}\text{Bi}$  radionuclides placed inside the cell nucleus. In particular, the radial distribution of deposited energy along the radius of cell nucleus was estimated, which is most important for directly tumoral cell killing. In our analysis, we also calculated the total lifetime of decay chain per decay, kinetic energy spectrum of the emitted electrons and total deposited energy per decay. Our simulations are in the concordance with the data indicating that  $^{213}\text{Bi}$  exhibits a shorter time of decay chain than  $^{125}\text{I}$ .

In our analysis, we performed the cluster analysis of spatial distribution of energy deposition from particles emitted inside the 2  $\mu\text{m}$ -diameter cell nucleus. In order to address the possibility of DNA damage, we calculated the frequency distribution of emitted particles using the cluster size of 2 nm, which corresponds to the diameter of the native double-stranded DNA helix. Our calculations demonstrate that for  $^{213}\text{Bi}$  the probability of ionization inside a cluster is higher than for  $^{125}\text{I}$ .  $^{213}\text{Bi}$  also exhibits the broader distribution of energy deposition in clusters than  $^{125}\text{I}$ .

Our study suggests that the package we use may be utilized in solving not only radiation research problems, but it also may have wide applications in educational and practical purposes.

## REFERENCES

1. *Amato E. et al.* Use of the Geant4 Monte Carlo to Determine Three-Dimensional Dose Factors for Radionuclide Dosimetry // Nucl. Instr. Meth. A. 2013. V. 708. P. 15–18.
2. *Campos L.* Dosimetry in Thyroid Follicles due to Low-Energy Electrons of Iodine Using the Monte Carlo Method // Radiol. Bras. 2008. V. 41. P. 403–407.
3. *Buscombe J.R.* Radionuclides in the Management of Thyroid Cancer // Cancer Imaging. 2007. V. 7. P. 202–209.

4. *Fondell A.* Two-Step Targeting for Effective Radionuclide Therapy: Preclinical Evaluation of  $^{125}\text{I}$ -Labelled Anthracycline Delivered by Tumour Targeting Liposomes / Digital Comprehensive Summaries of Uppsala Dissertations from the Faculty of Medicine 708. Uppsala: Acta Universitatis Upsaliensis, 2011. 100 p.
5. *Agostinelli S. et al.* Geant4 — A Simulation Toolkit // Nucl. Instr. Meth. A. 2003. V. 506. P. 250–303.
6. *Allison J. et al.* Geant4 Developments and Applications // IEEE Trans. Nucl. Sci. 2006. V. 53. P. 270–278.
7. *Li W.* Iodine-125 Induced DNA Strand Breakage: Contributions of Different Physical and Chemical Radiation Action Mechanisms. Technische Universität München, Dissertation, 2002.
8. *Booz J. et al.* Auger-Electron Cascades, Charged Potential and Microdosimetry of Iodine-125 // Radiat. Environ. Biophys. 1987. V. 26. P. 151–162.
9. *Li W.B. et al.* Track Structures and Dose Distributions from Decays of  $^{131}\text{I}$  and  $^{125}\text{I}$  in and around Water Spheres Simulating Micrometastases of Differentiated Thyroid Cancer // Radiat. Res. 2001. V. 156. P. 419–429.
10. *Toncova H.* Simulation of DNA Damages Induced by Incorporated  $^{125}\text{I}$ . Czech Technical University in Prague, Dissertation, 2005.
11. *Dadachova E.* Radioimmunotherapy of Infection with  $^{213}\text{Bi}$ -Labeled Antibodies // Curr Radiopharm. 2008. V. 1. P. 234–239.
12. *Tuli J.* Evaluated Nuclear Structure Data File // Nucl. Instr. Meth. A. 1996. V. 369. P. 506–510.
13. *Truscott P. et al.* Geant4 — A New Monte Carlo Toolkit for Simulating Space Radiation Shielding and Effects // Radiation Effects Data Workshop. Reno, NV, 2000. P. 147–152.
14. ICRU Report 86. Quantification and Reporting of Low-Dose and Other Heterogeneous Exposures // Journal of the ICRU. 2011. V. 11, No 2.
15. *Batmunkh M. et al.* Cluster Analysis of HZE Particle Tracks as Applied to Space Radiobiology Problems // Phys. Part. Nucl., Lett. 2013. V. 10, No. 7. P. 854–859.
16. *Brun R., Rademakers F.* ROOT — An Object-Oriented Data Analysis Framework // Nucl. Instr. Meth. A. 1997. V. 389. P. 81–86.
17. *Elmroth K., Stenerlow B.* DNA-Incorporated  $^{125}\text{I}$  Induces More than One Double-Strand Break per Decay in Mammalian Cells // Radiat. Res. 2005. V. 163. P. 369–373.

Received on June 16, 2014.

Редактор *В. В. Булатова*

Подписано в печать 02.09.2014.

Формат 60 × 90/16. Бумага офсетная. Печать офсетная.

Усл. печ. л. 0,81. Уч.-изд. л. 1,14. Тираж 205 экз. Заказ № 58322.

Издательский отдел Объединенного института ядерных исследований  
141980, г. Дубна, Московская обл., ул. Жолио-Кюри, 6.

E-mail: [publish@jinr.ru](mailto:publish@jinr.ru)

[www.jinr.ru/publish/](http://www.jinr.ru/publish/)